J|A|C|S
ARTICLES

Published on Web 10/07/2009

Hydrogen Storage Properties of Nanosized $MgH_2-0.1TiH_2$ Prepared by Ultrahigh-Energy−High-Pressure Milling

Jun Lu,[†] Young Joon Choi,[†] Zhigang Zak Fang,*[,†] Hong Yong Sohn,[†] and Ewa Rönnebro[‡]

Department of Metallurgical Engineering, University of Utah, 135 South 1460 East Room 412, Salt Lake City, Utah 84112-0114, and Pacific Northwest National Laboratory, 902 Battelle Boulevard, Richland, Washington 99352

Received July 28, 2009; E-mail: zak.fang@utah.edu

Abstract: Magnesium hydride (MgH_2) is an attractive candidate for solid-state hydrogen storage applications. To improve the kinetics and thermodynamic properties of MgH_2 during dehydrogenation−rehydrogenation cycles, a nanostructured $MgH_2-0.1TiH_2$ material system prepared by ultrahigh-energy−high-pressure mechanical milling was investigated. High-resolution transmission electron microscope (TEM) and scanning TEM analysis showed that the grain size of the milled $MgH_2-0.1TiH_2$ powder is approximately 5−10 nm with uniform distributions of TiH_2 among MgH_2 particles. Pressure−composition-temperature (PCT) analysis demonstrated that both the nanosize and the addition of TiH_2 contributed to the significant improvement of the kinetics of dehydrogenation and hydrogenation compared to commercial MgH_2. More importantly, PCT cycle analysis demonstrated that the $MgH_2-0.1TiH_2$ material system showed excellent cycle stability. The results also showed that the ΔH value for the dehydrogenation of nanostructured $MgH_2-0.1TiH_2$ is significantly lower than that of commercial MgH_2. However, the ΔS value of the reaction was also lower, which results in minimum net effects of the nanosize and the addition of TiH_2 on the equilibrium pressure of dehydrogenation reaction of MgH_2.

1. Introduction

Magnesium and magnesium-based alloys are considered attractive candidates as rechargeable hydrogen storage materials because of their high hydrogen capacities (theoretically up to 7.6 wt. %), reversibility, and low costs. Although of interest for stationary applications, a major impediment for practical use of MgH_2 for hydrogen storage related to fuel cell technology is that its equilibrium temperature at 1 bar hydrogen pressure is 288 °C, which is much higher than the fuel cell operation temperature of ca. 85 °C.[1] This is attributed to the fact that magnesium has very strong affinity to hydrogen and the decomposition enthalpy of MgH_2 is 75 kJ/mol H_2,[2−4] rendering the material thermodynamically too stable within the temperature range that is considered. In addition to the thermodynamic issues, the kinetics of dehydrogenation of MgH_2 is also slow at moderate temperatures. MgH_2 must be heated to 300−400 °C to achieve an adequate rate of dehydriding and hydriding, if no additives are used.

There are several possible approaches to improve the performance of MgH_2 for hydrogen storage. One of them is to alloy or dope with transition metal elements. For example, the dehydrogenation temperature of MgH_2 can be significantly reduced by alloying Mg with Ni because the Mg−H bonding energy is reduced by forming the intermetallic compound Mg_2Ni and its hydride.[5] However, because of the addition of transition metal Ni, Mg_2NiH_4 suffers from heavy penalty in loss of hydrogen storage capacity compared to MgH_2. Alternatively, a small percentage of catalytic transition elements, such as Ti, V, Mn, Fe, Co, Ni, Cu, Pd, and some of their oxides, may be added to improve dehydrogenation and hydrogenation without significantly reducing the hydrogen storage capacity.[6−15] One of the most notable reported studies was Ni^{nano}-doped MgH_2 composite prepared by mechanical milling, which showed substantially improved kinetics of dehydrogenation compared to undoped MgH_2.[14] In a different approach, several unknown

[†] University of Utah.
[‡] Pacific Northwest National Laboratory.

(1) IEA/DOE/SNL Hydride Database available at the Hydride Information Center, Sandia National Laboratories home page. http://hydpark.ca.sandia.gov/.
(2) Stampfer, J. F.; Holley, C. E.; Suttle, J. F. *J. Am. Chem. Soc.* **1960**, *82*, 3504.
(3) Bogdanovic, B.; Hartwig, T. H.; Spliethoff, B. *Int. J. Hydrogen Energy* **1993**, *18*, 575.
(4) Groll, M. *Int. J. Hydrogen Energy* **1994**, *19*, 507.
(5) Bogdanovic, B.; Hofmann, H.; Neuy, A.; Reiser, A.; Schlichte, K.; Spliethoff, B.; Wessel, S. *J. Alloys Compd.* **1999**, *292*, 57.
(6) Bowman, R. C., Jr.; Fultz, B. *MRS Bull.* **2002**, *27*, 688.
(7) Liang, G.; Huot, J.; Boily, S.; Neste, A. V.; Schulz, R. *J. Alloys Compd.* **1999**, *291*, 295.
(8) Song, M.-Y.; Mumm, D. R.; Kwon, S.-N.; Hong, S.-H.; Bae, J.-S. *J. Alloys Compd.* **2006**, *416*, 239.
(9) Reule, H.; Hirscher, M.; Weisshardt, A.; Kronmuller, H. *J. Alloys Compd.* **2000**, *305*, 246.
(10) Dehouche, Z.; Goyette, J.; Bose, T. K.; Huot, J.; Schulz, R. *Nano Lett.* **2001**, *1*, 175.
(11) Liang, G. *J. Alloys Compd.* **2004**, *370*, 123.
(12) De Castro, J. F. R.; Santos, S. F.; Costa, A. L. M.; Yavari, A. R.; Botta, W. J.; Ishikawa, T. T. *J. Alloys Compd.* **2004**, *376*, 251.
(13) Charbonnier, J.; de Rango, P.; Fruchart, D.; Miraglia, S.; Pontonnier, L.; Rivoirard, S.; Skryabina, N.; Vulliet, P. *J. Alloys Compd.* **2004**, *383*, 205.
(14) Hanada, N.; Ichikawa, T.; Fujii, H. *J. Phys. Chem. B* **2005**, *109*, 7188.
(15) Barkhordarian, G.; Klassen, T.; Bormann, R. *J. Phys. Chem. B* **2006**, *110*, 11020.

Mg_xTH_y compounds (T = Ti, V, Cr, Mn, or Nb) have been discovered, which were prepared by mixing MgH_2 with a transition metal or binary transition metal hydride and heating with a hydrogen source at GPa high pressures.[16−19] The dehydrogenation temperatures of these unknown compounds were lower as compared to MgH_2. Also, it has been reported that a thin film of metastable binary alloys of Mg and Ti (Mg_yTi_{1-y}, $0.5 \leq y \leq 0.95$) has an enhanced electrochemical hydrogenation property superior to that of a Mg film.[20] Inspired by this, we aimed at preparing Mg_xTiH_y in powder form by utilizing less extreme conditions, such as ball milling; however, our findings were unexpected, as we will further report here.

Mechanical ball milling, which is known to produce nanosized particles, is often used for improving hydrogen storage properties.[21−24] One of the earlier studies of ball milling commercial MgH_2 powders was undertaken by Hout et al.,[25] who pointed out that the particle size associated with the increase of specific surface area (SSA) was reduced, and also that nanosized grains were formed during ball milling. Since then, there has been a large number of studies reported on doped or undoped $Mg(H_2)$ by mechanical ball milling for improving the dehydrogenation and hydrogenation kinetics of MgH_2.[26−35] For example, Liang et al.[32] reported improved H_2-storage properties of MgH_2 with 5 mol % transition metals (Ti, V, Mn, Fe, and Ni) ball milled for 20 h, in which the composite with V released ~5 wt % hydrogen within 200 s at 300 °C. It is noted, however, that conventional ball milling typically produces micrometer-sized particles made up of crystal grains with a minimum size of about 15 nm.[26,27] During dehydrogenation−hydrogenation cycling, coarsening of particles and grain growth take place rapidly, leading to degradation of the hydrogenation−dehydrogenation properties and the cyclic stabilities from that of the milled material.[26]

Reactive ball milling of elemental metals or prealloyed intermetallic compounds under hydrogen has been shown to be useful because the formation of nanograins can take place simultaneously with the formation of a hydride,[36] significantly improving dehydrogenation and hydrogenation kinetics by eliminating the need for thermal activation.[37] Another advantage of reactive milling is that oxidation, which would most likely occur otherwise, can be minimized.

It should be emphasized, however, that it is generally agreed that mechanical milling does not have any significant effect on the thermodynamics of MgH_2; specifically the enthalpy of dehydrogenation of MgH_2 does not change,[32] although the use of mechanical milling and resultant nanosized particles were very effective for improving the kinetics of dehydrogenation and hydrogenation of MgH_2. Theoretical calculations, on the other hand, suggested that the dehydrogenation enthalpy for pure MgH_2 can be reduced in systems with physical confinement such as small crystallites or thin film.[38−42] Quantum-chemical calculations showed that if the crystallite size is reduced to below 2 nm, the absolute value of enthalpy decreases dramatically. For example, for 0.9 nm MgH_2 crystallites, the enthalpy of decomposition is only 63 kJ/K mol·H_2 and the theoretical equilibrium temperature at 1 bar hydrogen pressure is 200 °C.[40] It has also been predicted that encapsulation of MgH_2 in a nanosized scaffold can considerably lower the dehydrogenation temperature because of physical confinement.[41] Experimentally, Jongh et al.[43] reported a method to prepare large quantities of 3D carbon-supported metallic magnesium using melt infiltration. Crystallite sizes of Mg were on the order of a few nanometers. However, no thermodynamic data were given with respect to the dehydrogenation of MgH_2 in this nanoscaled material. Thus, finding a method to improve both kinetic and thermodynamic properties of MgH_2 without substantially reducing its hydrogen storage capacity remains a difficult challenge.

In our previous paper,[44] it was demonstrated that nanosized Mg−Ti−H systems synthesized using a custom-made ultrahigh-energy−high-pressure (UHEHP) mechanical milling machine enhanced dehydrogenation properties of MgH_2. The nanosized Mg−Ti−H materials exhibited a significantly lower dehydrogenation temperature than that of commercial MgH_2 (<250 °C). Subsequently, systematic investigations were carried out using thermal gravimetric analysis (TGA) and differential thermal analysis (DTA) to study the effects of TiH_2 content and milling time on the dehydrogenation behavior of Mg−Ti−H systems.[45] It was found that the decomposition temperature of MgH_2−TiH_2 mixtures varies as a function of the TiH_2 content. The lowest dehydrogenation onset temperature (~110 °C) based on TGA

(16) Kyoi, D.; Rönnebro, E.; Blomqvist, H.; Chen, J.; Kitamura, N.; Sakai, T.; Nagai, H. *Mater. Trans.* **2002**, *43*, 1124.
(17) Kyoi, D.; Rönnebro, E.; Kitamura, N.; Ueda, A.; Ito, M.; Katsuyama, S.; Sakai, T. *J. Alloys Compd.* **2003**, *361*, 252.
(18) Kyoi, D.; Sato, T.; Rönnebro, E.; Kitamura, N.; Ueda, A.; Ito, M.; Katsuyama, S.; Hara, S.; Noréus, D.; Sakai, T. *J. Alloys Compd.* **2004**, *372*, 213.
(19) Kyoi, D.; Sato, T.; Rönnebro, E.; Tsuji, Y.; Kitamura, N. *J. Alloys Compd.* **2004**, *375*, 253.
(20) Vermeulen, P.; Niessen, R. A. H.; Notten, P. H. L. *Electrochem. Commun.* **2006**, *8*, 27.
(21) Asano, K.; Enoki, H.; Akiba, E. *Mater. Trans.* **2007**, *48*, 121.
(22) Barkhordarian, G.; Klassen, T.; Bormann, R. *J. Phys. Chem. B* **2006**, *110*, 11020.
(23) Imamura, H.; Masanari, K.; Kusuhara, M.; Katsumoto, H.; Sumi, T.; Sakata, Y. *J. Alloys Compd.* **2005**, *386*, 211.
(24) Aguey-Zinsou, K. F.; Ares-Fernandez, J. R. *Chem. Mater.* **2008**, *20*, 376.
(25) Hout, J.; Liang, G.; Boily, S.; Van Neste, A.; Schulz, R. *J. Alloys Compd.* **1999**, *293−295*, 495.
(26) Zaluska, A.; Zaluski, L.; Ström-Olsen, J. O. *J. Alloys Compd.* **1999**, *288*, 217.
(27) Schimmel, H. H.; Hout, J.; Chapon, L. C.; Tichelaar, F. D.; Mulder, F. M. *J. Am. Chem. Soc.* **2005**, *127*, 14348.
(28) Lillo-Rodenas, M. A.; Aguey-Zinsou, K. F.; Cazorla-Amoros, D.; Linares-Solano, A.; Guo, Z. X. *J. Phys. Chem. C* **2008**, *112*, 5984.
(29) Schulz, R.; Hout, J.; Liang, G.; Boily, S.; Van Neste, A. *Mater. Sci. Forum* **1999**, *312−314*, 615.
(30) Schulz, R.; Hout, J.; Liang, G.; Boily, S.; Lalande, G.; Denis, M. C.; Dodelet, J. P. *Mater. Sci. Eng., A* **1999**, *267*, 240.
(31) Ares, J. R.; Aguey-Zinsou, K.-F.; Klassen, T.; Bormann, R. *J. Alloys Compd.* **2007**, *434−435*, 729.
(32) Liang, G.; Huot, J.; Boily, S.; Neste, A. V.; Schulz, R. *J. Alloys Compd.* **1999**, *292*, 247.
(33) Gennari, F. C.; Castro, F. J.; Urretavizcaya, G. *J. Alloys Compd.,* **2001**, *321*, 46.
(34) Hanada, N.; Ichikawa, T.; Orimo, S.-I.; Fujii, H. *J. Alloys Compd.* **2004**, *366*, 269.
(35) Mulas, G.; Schiffini, L.; Tanda, G.; Cocco, G. *J. Alloys Compd.* **2005**, *404−406*, 343.
(36) Hout, J.; Akiba, E. *J. Alloys Compd.* **1995**, *231*, 815.
(37) Orimo, S.-I.; Fujii, H. *J. Alloys Compd.* **1996**, *232*, L16.
(38) Liang, J. J.; Kung, W. C. *J. Phys. Chem. B* **2005**, *109*, 17837.
(39) Berube, V.; Radtke, G.; Dresselhaus, M.; Chen, G. *Int. J. Hydrogen Res.* **2007**, *31*, 637.
(40) Wagemans, R. W. P.; van Lenthe, J. H.; de Jongh, P. E.; van Dillen, A. J.; de Jong, K. P. *J. Am. Chem. Soc.* **2005**, *127*, 16675.
(41) Liang, J. J. *Appl. Phys. A: Mater. Sci. Process.* **2005**, *80*, 173.
(42) Cheung, S.; Deng, W.-Q.; van Duin, A. C. T.; Goddard, W. A. *J. Phys. Chem. A* **2005**, *109*, 851.
(43) de Jongh, P. E.; Wagemans, R. W. P.; Eggenhuisen, T. M.; Dauvillier, B. S.; Radstake, P. B.; Meeldijk, J. D.; Geus, J. W.; de Jong, K. P. *Chem. Mater.* **2007**, *19*, 6052.
(44) Choi, Y. J.; Lu, J.; Sohn, H. Y.; Fang, Z. Z. *J. Power Sources* **2008**, *180*, 491.
(45) Choi, Y. J.; Lu, J.; Sohn, H. Y.; Fang, Z. Z.; Ronnebro, E. *J. Phys. Chem. C*, in press.

analysis was achieved when the MgH_2:TiH_2 molar ratio was 10:1.[45] This is an encouraging result, indicating that the MgH_2-TiH_2 mixture has favorable dehydrogenation properties compared to MgH_2 by itself. The mechanisms or underlying reasons for the reduction of the dehydrogenation temperature of MgH_2 by TiH_2 and UHEHP milling are, however, still not well understood. In particular, the effects of nanosize and addition of TiH_2 on thermodynamics of dehydrogenation of MgH_2, if any, are still not clear, nor the effects of UHEHP milling and the addition of TiH_2 on the kinetics of hydrogen storage reactions compared to undoped MgH_2. In order to clarify this, we here present thermodynamic and kinetic properties of nanosized $MgH_2-0.1TiH_2$ as investigated using a Sieverts type pressure−composition−temperature (PCT) gas−solid reaction instrument. The dehydrogenation−hydrogenation isotherms and cyclic behavior were analyzed. Transmission electron microscopy (TEM) was used to characterize the size of nanoparticles and the distribution of TiH_2.

2. Experimental Apparatus and Procedure

The raw materials for this work, magnesium hydride (MgH_2, 98%) and titanium hydride (TiH_2, 99%), were purchased from Sigma-Aldrich (Milwaukee, WI) and Alfa-Aesar (Ward Hill, MA), respectively, and used as received without any further purification. Note that the impurities content of the raw material is significant, which would result in lower than theoretical content of hydrogen in the raw material. All the material handling was carried out in a glovebox filled with purified argon (99.999%), which can keep a low water vapor concentration (less than 1 ppm) and a low oxygen concentration (less than 1 ppm) by a recycling purification system in the presence of an oxygen scavenger and a drying agent to prevent raw materials and samples from oxidation and/or hydroxide formation. Five grams of the mixtures of MgH_2 and TiH_2 in a ratio of 10:1 were milled using a custom-made ultrahigh-energy−high-pressure (UHEHP) ball milling device under 13.8 MPa hydrogen pressure. The balls to powder ratio was 35:1 by weight, and the milling time was 4 h at room temperature.

The hydrogen release−uptake properties of the milled mixtures $MgH_2-0.1TiH_2$ were evaluated by using a commercial Sieverts type apparatus (PCTPro-2000) upon heating to 300 °C at a heating rate of 5 °C/min. About 1.5 g of the milled sample is loaded into a stainless steel container as loosely packed powder, which is then sealed to the PCT autoclave in the glovebox. Hydrogen pressures were measured by a Teledyne Taber model 206 piezoelectric transducer, 0−20 MPa, with a resolution of 10^{-4} MPa. During dehydrogenation−hydrogenation, the sample temperature and applied pressure were monitored and recorded by a Lab View-based software program. The amount of hydrogen release−uptake was calculated by the pressure changes in calibrated volumes, of which the details are described elsewhere.[46]

The identification of particle sizes and phases in the reactants and products before and after the PCT measurements was carried out using an X-ray diffractometer (XRD, Siemens D5000) with Ni-filtered Cu Kα radiation ($\lambda = 1.5406$ Å). Each sample for XRD analysis was mounted on a glass slide and covered with a Kapton tape as a protective film in the glovebox. The X-ray intensity was measured over diffraction angle 2θ from 10° to 100° with a scanning rate of 0.02°/s. On the basis of XRD peak broadening, the crystallite size and effective internal strain of sample were estimated using the Stokes and Wilson formula, as described in the following equation.[47]

$$\beta = \beta_d + \beta_\varepsilon = \frac{0.89\lambda}{d\cos\theta} + 4\varepsilon\tan\theta \quad (1)$$

where β is full width at half-maximum (fwhm) of the diffraction peak after instrument correction; β_d and β_ε are fwhm caused by small grain size and internal stress, respectively; and d and ε are grain size and internal stress or lattice distortion. On the basis of eq 1, the average crystallite sizes of MgH_2 in the milled $MgH_2-0.1TiH_2$ powder were calculated as about 5 nm.[45]

A field-emission gun scanning electron microscope (FEI Quanta 600 FEG) was employed to observe the morphology and estimate the particle size of the samples. The samples were protected from exposure to air during the transfer to the SEM sample chamber by a conductive tape applied in the glovebox. To obtain more accurate estimates of the particle sizes and or crystallite sizes, a transmission electron microscope (TEM, FEI Tecnai 30) with an accelerating voltage of 300 kV was employed. To analyze the distribution of TiH_2, a scanning transmission electron microscope (STEM, FEI Tecnai 20) equipped with energy dispersive X-ray spectrometry (EDS) was used. To prepare a specimen for TEM or STEM observations, a dilute suspension was dropped onto a copper grid and dried. The results of the TEM observations confirmed that the crystallite size of the milled $MgH_2-0.1TiH_2$ composite powder was indeed approximately 5 to 10 nm.

3. Results

First, it should be pointed out that, regarding the milled material, there were no indications of the formation of any metastable ternary Mg−Ti−H phases under the current experimental conditions based on XRD analysis,[45] which is consistent with our previous work.[44] Therefore, the material that was subjected to hydrogen release and uptake reactions in this study is regarded as nanostructured uniformly dispersed mixtures of MgH_2 and TiH_2.[45] In principle, both MgH_2 and TiH_2 contained in the mixtures can be dehydrogenated according to the following equations:

$$MgH_2 = Mg + H_2 \quad (2)$$

$$TiH_2 = Ti + H_2 \quad (3)$$

However, reaction 3 takes place only when the temperature is higher than 400 °C, which is higher than the maximum temperature of 300 °C used in this study. XRD results confirmed that the TiH_2 phase remained as a separate hydride phase before and after dehydrogenation procedures and measurements.[44,45] Therefore, the following results and discussions are primarily presented in the context of reaction 2.

3.1. Cyclic Stability of Dehydrogenation−Hydrogenation of the Milled $MgH_2-0.1TiH_2$ System. One of the most significant and important findings of this study is that the milled $MgH_2-0.1TiH_2$ material shows an excellent cyclic stability upon hydrogenation−dehydrogenation tests. Cyclic kinetic measurements of dehydrogenation and hydrogenation were carried out using the PCT instrument according to the following procedures: dehydrogenation was performed by keeping the mixture at 300 °C under 1 kPa H_2 for 1 h, while hydrogenation was performed at 300 °C for 1 h under a H_2 pressure of about 2 MPa, which is substantially higher than the equilibrium pressure. Between the dehydrogenation and hydrogenation of each cycle, a 30-min evacuation process was conducted to ensure the complete dehydrogenation of the sample. A total of 80 cycles were performed, and the results are presented in Figure 1, showing that there was little loss in hydrogen storage capacity after 80 cycles and indicating that the $MgH_2-0.1TiH_2$ nanocomposite

(46) Luo, W.; Clewley, J. D.; Flanagam, T. B. *J. Less-Common Met.* **1988**, *141*, 103.
(47) Williamson, G. K.; Hall, W. H. *Acta Metall.* **1953**, *1*, 22.

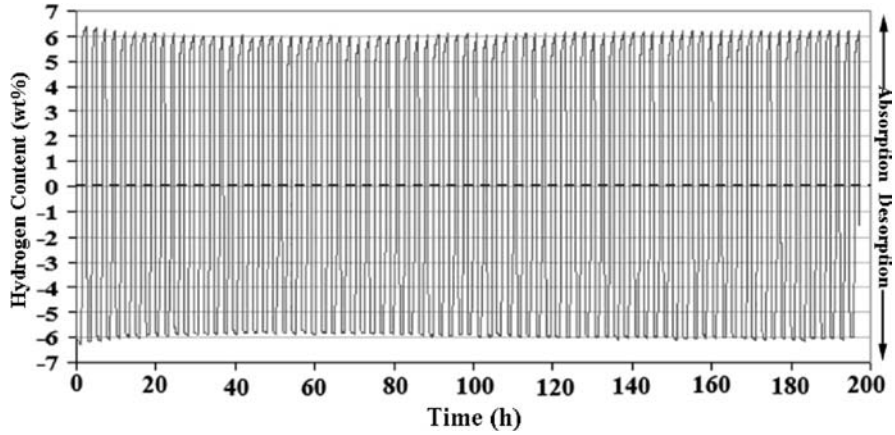

Figure 1. Cyclic kinetics measurements of the milled $MgH_2-0.1TiH_2$ at 300 °C.

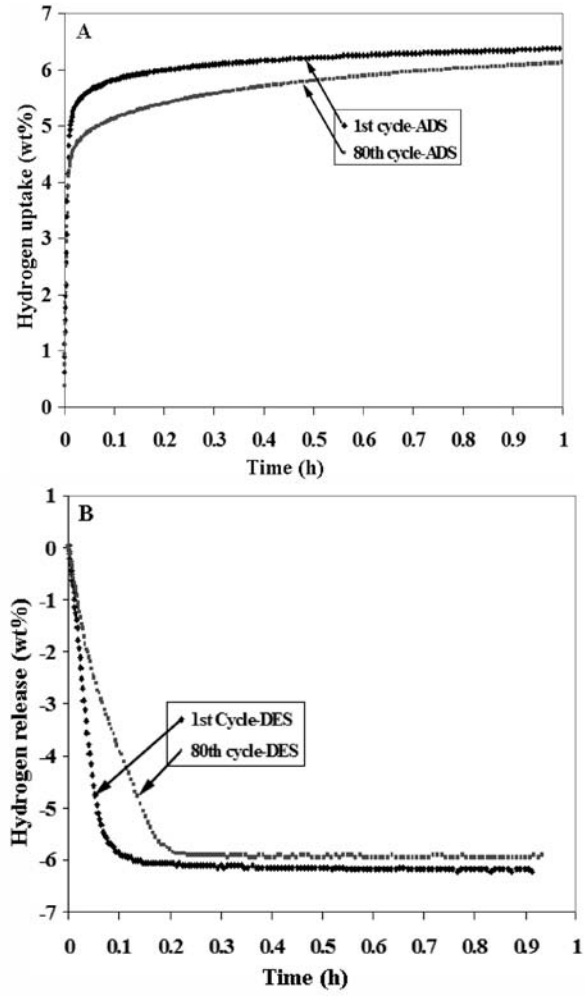

Figure 2. (A) Isothermal dehydrogenation curves for the milled $MgH_2-0.1TiH_2$ under 1 kPa hydrogen pressure at 300 °C during the 1st and 80th cyclic kinetics measurements, respectively. (B) Isothermal hydrogenation curves for the dehydrogenated $MgH_2-0.1TiH_2$ under 2 MPa hydrogen pressure at 300 °C during the 1st and 80th cyclic measurements, respectively.

material system has excellent cycle stability. The kinetic data of the first and last cycles from the cyclic measurements were extracted and plotted as shown in Figures 2A and 2B. It is obvious that the kinetics of both hydrogenation and dehydrogenation remained intact from the first to the last cycle. Thus,

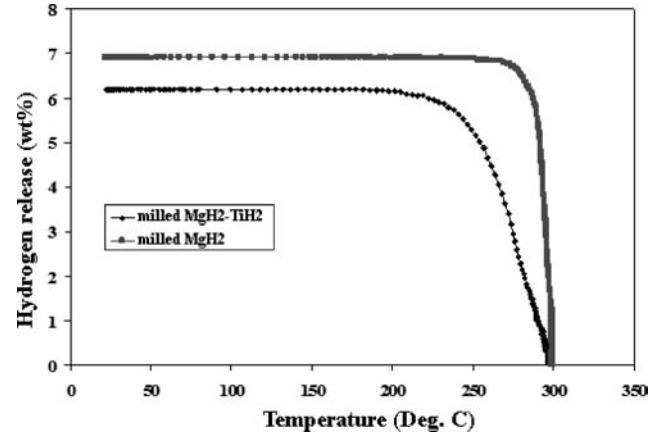

Figure 3. Temperature-programmed desorption (TPD) profiles for the milled $MgH_2-0.1TiH_2$ and milled pure MgH_2.

in this respect, $MgH_2-0.1TiH_2$ is superior to undoped nano- or microscaled MgH_2, which loses its hydrogen storage capacity during cycling.[26]

3.2. Dehydrogenation and Hydrogenation Kinetics of the Milled $MgH_2-0.1TiH_2$ System. In order to further investigate hydrogen storage properties of the milled $MgH_2-0.1TiH_2$ material, dehydrogenation and hydrogenation measurements under different conditions were performed using PCT, and the detailed results are given below.

Temperature-programmed desorption (TPD) and temperature-programmed adsorption (TPA) are common techniques for surveying the overall hydrogen storage behavior of solid hydride materials. During TPD or TPA, temperature is ramped up at a constant heating rate. The pressure changes during the temperature ramping is measured and converted to corresponding percentages of hydrogen release or uptake. Figure 3 shows the TPD profiles of the milled $MgH_2-0.1TiH_2$ and the milled pure MgH_2. First, both materials after UHEHP milling showed a drastically faster dehydrogenation rate than that of as-received commercial MgH_2, which released less than 0.5 wt % hydrogen by the same measurement.[28] This result confirms again that nanosized particles improves the kinetics of dehydrogenation of MgH_2, as reported in literature.[26,27] Figure 3 also shows that the dehydrogenation of the milled $MgH_2-0.1TiH_2$ started at about 180 °C, much lower than that of the milled undoped MgH_2 (280 °C). This suggests that dehydrogenation kinetics of MgH_2 was further improved by the addition of TiH_2, given that the particle sizes of both samples were similar after milling as shown

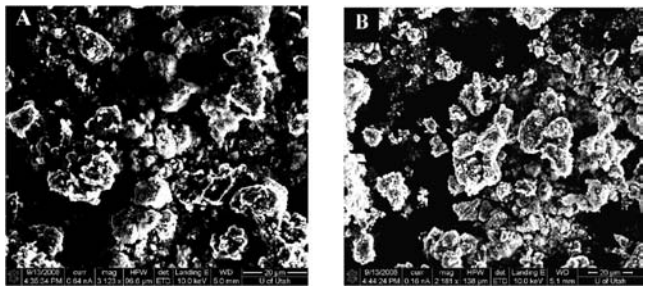

Figure 4. HR-SEM micrographs of the samples after UHEHP milling for 4 h: (A) MgH_2, and (B) $MgH_2-0.1TiH_2$, respectively.

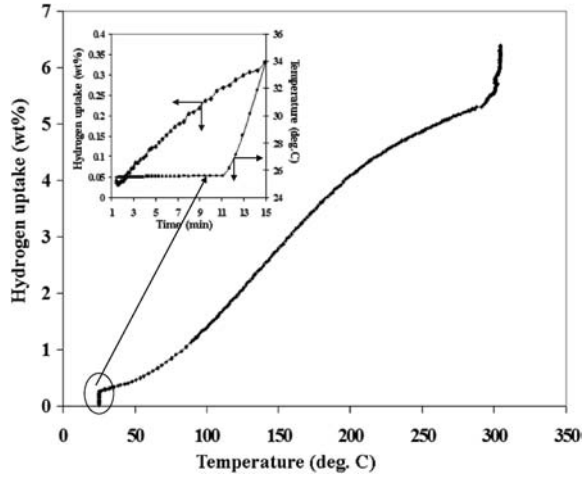

Figure 5. Temperature-programmed adsorption (TPA) profile for the dehydrogenated $MgH_2-0.1TiH_2$ under 2 MPa hydrogen pressure.

in Figure 4. A total of 6.20 wt % hydrogen was released from the milled $MgH_2-0.1TiH_2$ sample during the TPD experiment, which is slightly lower than its theoretical capacity (6.45 wt % considering only MgH_2 mixed with TiH_2, which does not decompose at the temperature measured). The less than maximum desorption is attributed to the impurities in the raw materials and the artificially set point of termination of the experiment due to the sluggish kinetics of desorption near the end of a cycle.

After dehydrogenation, the sample was exposed to 2 MPa of hydrogen pressure for the hydrogenation measurements. The TPA profile (Figure 5) of the dehydrogenated $MgH_2-0.1TiH_2$ sample shows that a total of 6.3 wt % hydrogen was recovered, suggesting that all Mg was rehydrogenated. Surprisingly, it was found that the hydrogenation started at room temperature (see inset TPA curve of Figure 5). More specifically, when the hydriding time at room temperature was prolonged, more hydrogen was absorbed, i.e., ca. 4 wt % in 4 h as shown in Figure 6. To the authors' best knowledge, this is the first time that hydrogenation of Mg in powder form has been observed at room temperature.[48] Clearly, the kinetics of hydrogenation of the $MgH_2-0.1TiH_2$ system is significantly improved compared to that of commercial MgH_2.

In addition to TPD and TPA, *isothermal dehydrogenation and hydrogenation measurements* were carried out to further investigate the kinetics of the dehydriding and hydriding reactions of $MgH_2-0.1TiH_2$. The dehydrogenation kinetics of

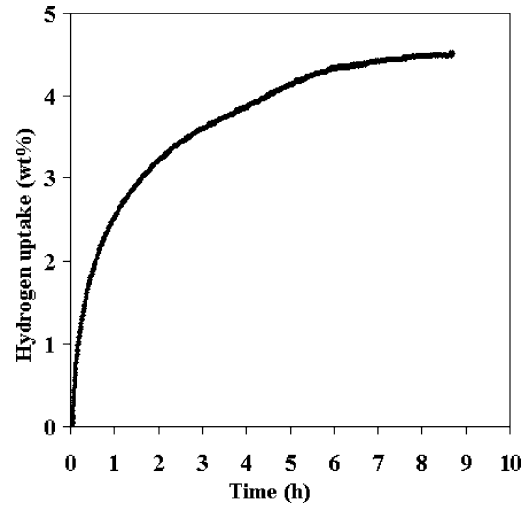

Figure 6. Isothermal hydrogenation curve for the dehydrogenated $MgH_2-0.1TiH_2$ under 2 MPa hydrogen pressure at room temperature.

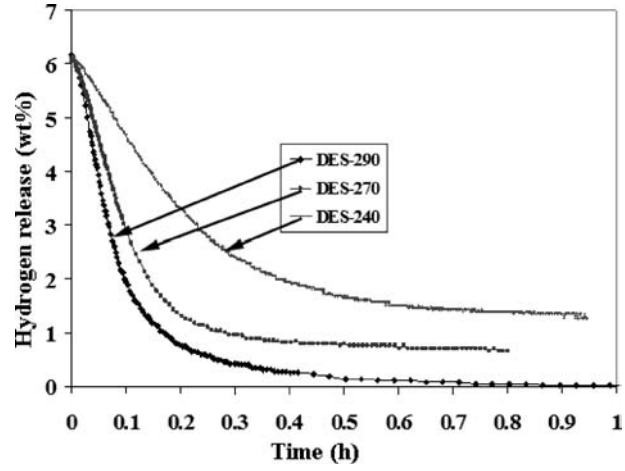

Figure 7. Isothermal dehydrogenation curves for the milled $MgH_2-0.1TiH_2$ under 1 kPa hydrogen pressure at 240, 270, and 290 °C, respectively.

$MgH_2-0.1TiH_2$ were characterized at 240, 270, and 290 °C under 0.1 kPa of hydrogen, respectively, while the hydrogenation kinetics of the dehydrogenated $MgH_2-0.1TiH_2$ were characterized at 210, 240, 270, and 290 °C under 2 MPa of hydrogen, respectively.

Figure 7 shows the isothermal dehydrogenation curves of the milled $MgH_2-0.1TiH_2$ at different temperatures. As expected, dehydrogenation is relatively sluggish at lower temperatures. It is still noted, however, that around 4 wt % hydrogen can be released at 240 °C in 20 min. The effect of temperature on dehydrogenation kinetics of MgH_2 has been previously reported for nickel-based catalysts, as well as for other materials.[32,49,50] By comparing current results on the kinetics of isothermal dehydrogenation of MgH_2 with available data in the literature, it can be shown that dehydrogenation kinetics is significantly improved by the use of UHEHP milling and the addition of TiH_2.

The improved kinetics can be further understood by calculating the activation energy of the dehydrogenation reaction of

(48) de Rango, P.; Chaise, A.; Charbonnier, J.; Fruchart, D.; Jehan, M.; Marty, Ph.; Miraglia, S.; Rivoirard, S.; Skryabina, N. *J. Alloys Compd.* **2007**, *52−57*, 446.

(49) Varin, R. A.; Czujko, T.; Wasmund, E. B.; Wronski, Z. S. *J. Alloys Compd.* **2007**, *423*, 217.

(50) Varin, R. A.; Czujko, T.; Wasmund, E. B.; Wronski, Z. S. *J. Alloys Compd.* **2007**, *446−447*, 63.

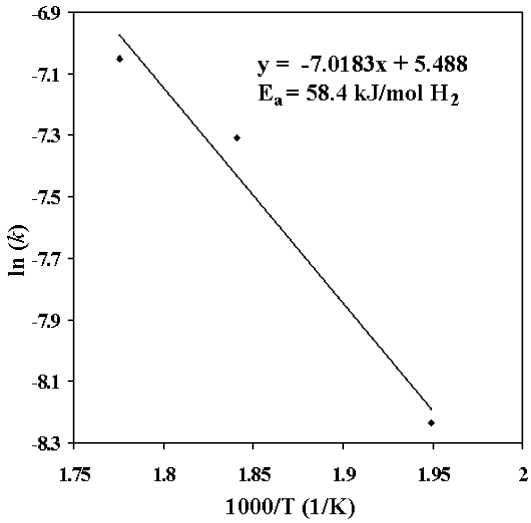

Figure 8. Kissinger plot of the milled $MgH_2-0.1TiH_2$ sample.

MgH_2. The activation energy for dehydrogenation of MgH_2 in the milled $MgH_2-0.1TiH_2$ has been calculated according to the Arrhenius equation as

$$E_A = -RT \ln\left(\frac{k}{k_0}\right) \tag{4}$$

where E_A is the activation energy, k is a temperature-dependent reaction rate constant, R is the gas constant, and T is the absolute temperature. The activation energy of the reaction can be determined by measuring the rate constant k at several different temperatures and then plotting $\ln(k)$ versus $1/T$ based on the following equation:

$$k = \frac{\frac{d\alpha}{dt}}{f(\alpha)} \tag{5}$$

where $f(\alpha)$ is a conversion function dependent on the reaction mechanism. Several solid-state reaction mechanism models have been tested to select the best fitting form, including the nucleation-and-growth, the geometric contraction, the diffusion, and the reaction order models based on the different geometry of the particles and the different driving forces. The function based on geometric contracting volume (R3 model) given below gave the best results:

$$kt = 1 - (1 - \alpha)^{1/3} \tag{6}$$

From the data in Figure 7, the activation energy (E_a) for dehydrogenation of MgH_2 in $MgH_2-0.1TiH_2$ is calculated as 58.4 kJ/mol H_2, as shown in Figure 8. This value agrees with the value that was calculated based on TGA analysis using the Ozawa−Flynn−Wall method and is much lower than that of undoped milled MgH_2 (96 kJ/mol H_2) and as-received commercial MgH_2 (135 kJ/ mol H_2).[44]

Figure 9 shows the isothermal hydrogenation curves of the dehydrogenated $MgH_2-0.1TiH_2$ at different temperatures. It can be seen that the dehydrogenated sample exhibited a very fast rate of adsorption at all temperatures measured. About 5 wt % of H_2 (>80% of total capacity) was absorbed in less than 1 min when the temperature is higher than 240 °C.

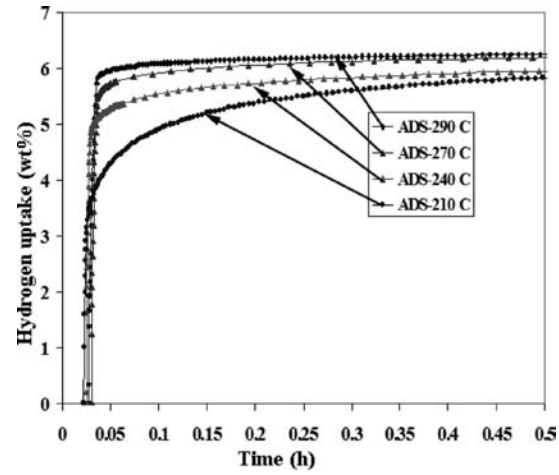

Figure 9. Isothermal hydrogenation curves for the dehydrogenated $MgH_2-0.1TiH_2$ under 2 MPa hydrogen pressure at 210, 240, 270, and 290 °C, respectively.

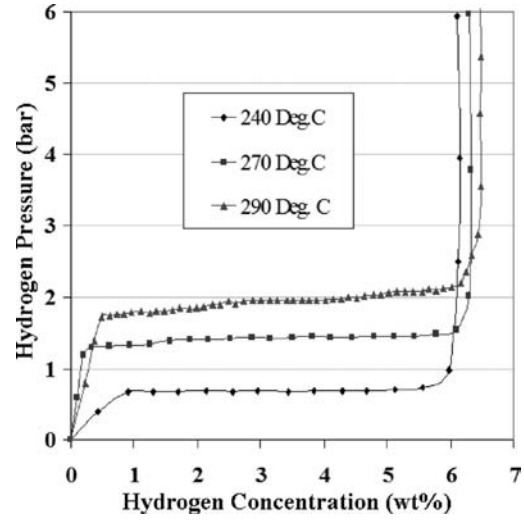

Figure 10. Pressure−composition−isothermal curves of the milled $MgH_2-0.1TiH_2$ at 240, 270, and 290 °C, respectively.

3.3. Pressure−Composition-Isothermal Measurements of the Milled $MgH_2-0.1TiH_2$ System. Pressure−composition−isothermal (PCI) experiments were carried out to study the thermodynamics of the $MgH_2-0.1TiH_2$ system. The reaction enthalpy (ΔH) and entropy (ΔS) for the dehydrogenation reaction were obtained by performing PCI runs at 240, 270, and 290 °C, as shown in Figure 10. The corresponding van't Hoff plots derived from the dehydrogenation PCI runs are plotted in Figure 11, together with those for dehydrogenation of commercial undoped MgH_2 which are well documented, in order to illustrate the effects of nanosize and the addition of TiH_2. These data are available in the open literature including the Sandia National Laboratory's database.[2−4] The calculated van't Hoff plot of dehydrogenation of MgH_2 using a commercial thermodynamics software (HSC) is also included in Figure 11 for comparison. Using the following equation, the reaction enthalpy and entropy were calculated and are listed in Table 1.

$$\ln P = \frac{\Delta H}{RT} - \frac{\Delta S}{R} \tag{7}$$

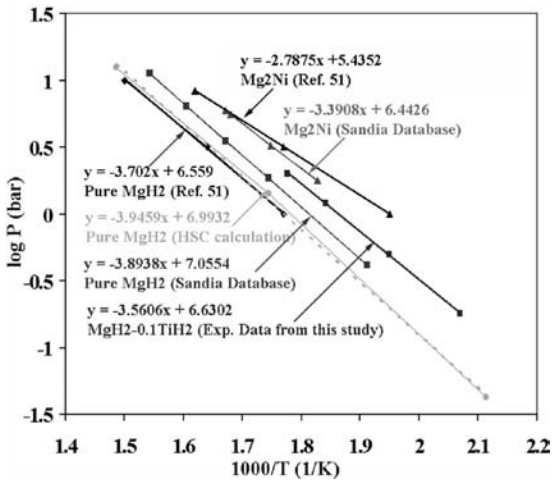

Figure 11. van't Hoff plot of the milled $MgH_2-0.1TiH_2$ system derived from the dehydrogenation PCI measurements and van't Hoff plot of MgH_2 based on the literature data.

Table 1. Reaction Enthalpy and Entropy for the Reactions of Mg + H_2 = MgH_2 and Mg_2Ni + $2H_2$ = Mg_2NiH_4 from Different Sources

systems	ΔH (kJ/K mol H_2)	ΔS (J/mol H_2)
pure MgH_2, Sandia National Lab database	−74.6	−135
pure MgH_2, ref 51	−70.8	−126
pure MgH_2, HSC calculation	−75.6	−134
$MgH_2-0.1TiH_2$, experimental data from this study	−68.2	−127
Mg_2Ni, Sandia National Lababoratory database	−64.9	−123
Mg_2Ni, ref 51	−53.4	−104

Comparing the results of this study, it appears that the equilibrium pressure for $MgH_2-0.1TiH_2$ is slightly higher than that of commercial MgH_2. However, the differences are small considering that the experimental measurement errors are on the same order of magnitude as these differences.

The data in Table 1 do show, however, that there are significant changes in reaction enthalpy. The ΔH for the dehydrogenation of $MgH_2-0.1TiH_2$ is 68 kJ/mol H_2, lower than that of the standard value for MgH_2 (75 kJ/mol H_2).[2−4] This is an unexpected finding because most published studies of MgH_2 have shown that it is very difficult to change the thermodynamics of dehydrogenation of MgH_2.[32] To further verify the changes of ΔH, differential thermal analysis (DTA) were performed on a series of samples to measure ΔH of dehydrogenation and to confirm the validity of the PCI results. These samples were: UHEHP milled $MgH_2-0.1TiH_2$, UHEHP milled MgH_2, and as-received commercial MgH_2. ΔH was calculated by integrating the DTA peaks shown in Figure 12 and listed in Table 2. The results indicate that the ΔH of the dehydrogenation reaction of $MgH_2-0.1TiH_2$ is 69 kJ/mol H_2, agreeing with the results of PCI measurements. From the DTA curves, it can also be seen that the milled $MgH_2-0.1TiH_2$ has a lower peak temperature than those of milled MgH_2 and commercial MgH_2. This indicates that the thermodynamics of the dehydrogenation reaction of the milled $MgH_2-0.1TiH_2$ is indeed different from MgH_2.

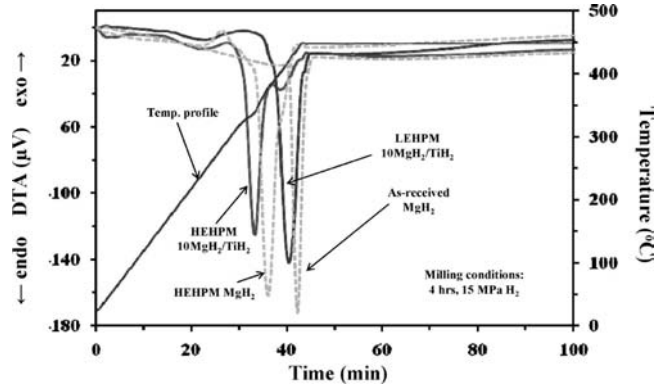

Figure 12. DTA profiles of the different samples containing MgH_2.

Table 2. Reaction Enthalpies of the Dehydrogenation of MgH_2 from the Different Samples, Which Were Calculated Based on the DTA Analysis

systems	ΔH (kJ/K mol H_2)
UHEHP milled $MgH_2-0.1TiH_2$	68.5 ± 1.0
UHEHP milled MgH_2	73.0 ± 1.4
LEHP milled $MgH_2-0.1TiH_2$	73.2 ± 0.8
as-received MgH_2	76.3 ± 1.5

Under the common assumption that ΔS is constant during the dehydrogenation of metal hydrides,[51,52] P_{eq} is expected to change significantly as ΔH value changes, which was, as shown above, not observed in this study. This apparent disagreement can be explained by allowing ΔS values to change. The data in Table 1 shows that the decrease in ΔS values had an opposite effect on P_{eq} as that of ΔH. The interpretation and the implications of recognizing the changes in ΔS values are further discussed in the next section.

4. Discussions

4.1. Effects of Nanosize and TiH_2 on the Thermodynamics of Dehydrogenation and Hydrogenation of $MgH_2-0.1TiH_2$. As shown here, the changes in the thermodynamics of the interaction of hydrogen with magnesium can be attributed to two factors: nanosize and the addition of TiH_2. First, the grain size of the materials investigated in this study is 5−10 nm, well below that of samples reported in the literature.[26,27] Theoretical studies have reported that using nanoparticles instead of bulk or coarse particles of hydrides can alter the thermodynamics of hydrogen uptake and release.[38−42] The thermodynamics of the process is governed by energy differences between the metal and its hydride. Because the energies (on a molar basis) of both reactants and products change going from bulk materials to nanosized particles, the reaction thermodynamics will be affected by the size of the grains. Second, the addition of TiH_2 into the system may also change the reaction thermodynamics of MgH_2 by weakening the Mg−H bond. This is consistent with theoretical predictions by Song et al.,[53] who demonstrated that the addition of Ti into the magnesium hydride matrix would lead to the decrease of the reaction enthalpy (ΔH) by using first principle simulation methods.

A common practice is to assume that the entropy contribution to metal hydride reactions is approximately 130 J/mol

(51) Yamaguchi, M.; Akiba, E. In *Electronic and Magnetic Properties of Metals and Ceramic Part II*; Buschow, K. H. J., Ed.; VCH: Weinheim, 1994; Vol. 3B, p 333.

(52) Züttel, A.; Wenger, P.; Rentsch, S.; Sudan, P.; Mauron, P.; Emmenegger, C. *J. Power Sources* **2003**, *118*, 1.

(53) Song, Y.; Guo, Z. X.; Yang, R. *Mater. Sci. Eng., A* **2004**, *365*, 73.

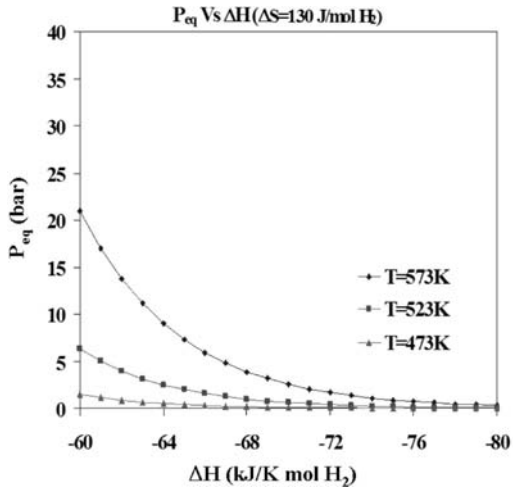

Figure 13. Plot of P_{eq} as a function of ΔH at different temperatures with a constant ΔS (ΔS = 130 J/K mol H_2).

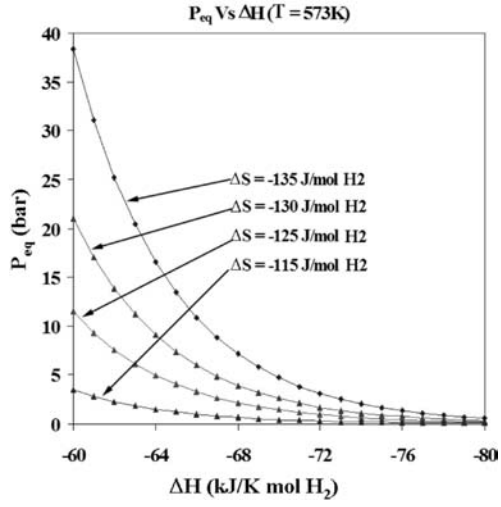

Figure 14. Plot of P_{eq} as a function of ΔH at different ΔS values with a constant temperature (T = 573 K).

H_2 for most simple metal−hydrogen systems.[50,51] It has been proposed that entropy change (ΔS) is primarily attributed to the loss of standard entropy of hydrogen gas as it enters the metal lattice.[51] Therefore, the entropy term does not have a strong dependence on the nature of the metal and could be considered constant. According to this assumption, Figure 13 shows a plot of P_{eq} as a function of ΔH at a constant ΔS (130 J/K mol H_2). It is seen that when ΔS is a constant, P_{eq} should increase as ΔH decreases. This general trend, however, is not supported by the published data on MgH_2, Mg_2NiH_4, or other metal hydrides. To fit experimental data of P_{eq} versus $1/T$, ΔS must also change, which is what the van't Hoff plots of this study demonstrates (Figure 11). To further examine the effect of ΔS on the equilibrium pressure, P_{eq} as a function of ΔH at different ΔS values are plotted in Figure 14. It can be seen that P_{eq} varies significantly with the change in ΔS value, which suggests that to understand the thermodynamics changes of MgH_2-TiH_2 compared to that of MgH_2, the changes in ΔS values cannot be ignored. Because the entropy value of the H_2 gas is constant, the changes in ΔS can only be accounted for by the differences in entropy between $MgH_2-0.1TiH_2$ and MgH_2. The fact that the ΔS as well as ΔH values changed from those of MgH_2 implies that TiH_2 has formed an alloy or solid solution with MgH_2 during the UHEHP milling, for which we do not yet have any direct evidence. Needless to say, further in-depth research is needed to fully understand the effects of TiH_2. Moreover, it should be noted that the measured enthalpy (ΔH = 69.8 kJ/K mol H_2) and entropy (ΔS = 129 J/mol H_2) for the hydrogenation reaction of the milled $MgH_2-0.1TiH_2$ system are slightly different from those of the dehydrogenation reaction. This suggests that the detailed mechanisms of hydrogenation may be different from that of the dehydrogenation, which is another subject that requires further study.

4.2. Effects of Nanosize and TiH_2 on the Kinetics of Dehydrogenation and Hydrogenation of $MgH_2-0.1TiH_2$. Another important aspect of the experimental results from this study is that the dehydrogenation and hydrogenation kinetics of $MgH_2-0.1TiH_2$ system is considerably improved compared to that of UHEHP milled MgH_2 and commercial MgH_2 materials which are coarse powders (approximately 35 μm in size). Such kinetic effects can also be understood qualitatively based on the effects of nanosize and the addition of TiH_2. The hydrogenation of magnesium is typically described as involving the following five steps:[27] (1) Hydrogen gas permeation through the particle bed; (2) surface adsorption and hydrogen dissociation; (3) migration of hydrogen atoms from the surface into Mg/MgH_2; (4) nucleation and growth of the hydride phase; (5) diffusion into the bulk. The second step is known to be rate-controlling since the addition of catalysts for this process increases the kinetics drastically. The third and fifth steps will, similar to the second step, scale with the surface area and size of the particles, respectively. As expected, nanosize of the particles increases the surface area per unit mass, which would obviously contribute to increase the rate of the reaction.[54]

The effect of TiH_2 on the kinetic process is not well understood. First, TiH_2 appears to act as a catalyst for the dehydrogenation and hydrogenation processes in the present system, considering that the second step is rate controlling. Nanocrystalline TiH_2 contained in the mixture could provide active catalytic sites for surface adsorption and hydrogen dissociation, which improves the kinetics of the hydrogenation of magnesium. The observation of hydrogenation by magnesium at room temperature in this mixture is an indirect evidence of that. Second, results of TEM observations (Figure 15) show that TiH_2 is uniformly distributed in the mixture. Therefore it is reasonable to assume that TiH_2, as a hydrogen-saturated catalyst, is in close contact with Mg particles and may act as nucleation and growth centers of the magnesium hydride phase as proposed by Schimmel et al.[27] Third, the uniformly doped TiH_2 could act as channels for dissociated hydrogen adatoms to spill over into the Mg matrix. It should be pointed out that, on the basis of our previous study, other Ti species, such as $TiCl_3$, do not exhibit a similar level of effects on hydrogen storage properties of MgH_2.[44]

Further, in addition to the catalytic effects, TiH_2 may also act as a grain growth inhibitor that prevents the coarsening of Mg or MgH_2 particles during the dehydriding−hydriding measurements. Figure 15 is a high-resolution TEM images of the milled sample and the sample after 80 cycles of hydrogena-

(54) Lin, C.; Xu, T.; Yu, J.; Ge, Q.; Xiao, Z. *J. Phys. Chem. C* **2009**, *113*, 8513–8517.

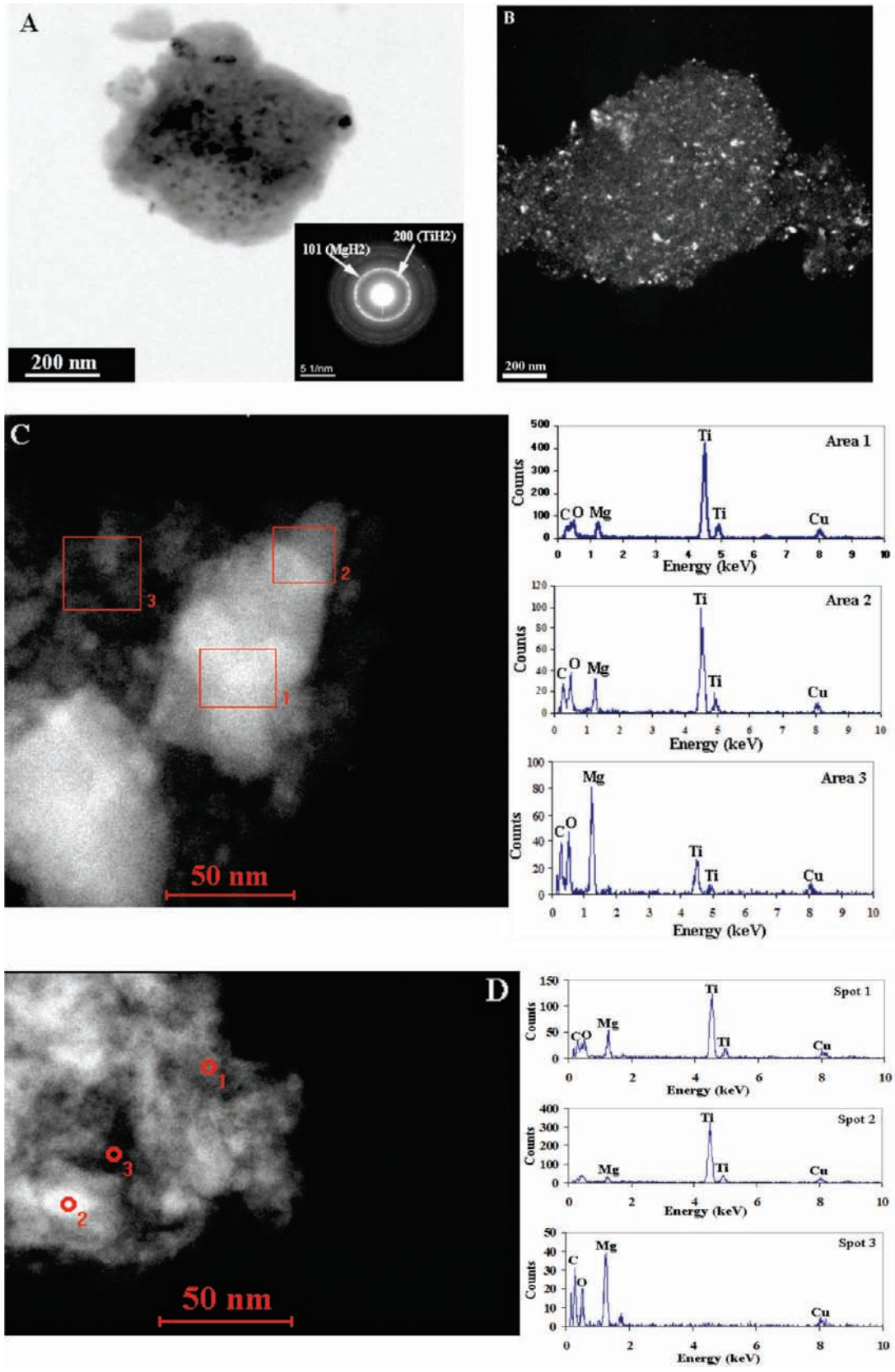

Figure 15. TEM micrographs of a mixture of $MgH_2-0.1TiH_2$ after UHEHP milling for 4 h: (A) bright-field image; (C) STEM image and EDS profile. TEM micrographs of a mixture of $MgH_2-0.1TiH_2$ after 80 cyclic measurements: (B) dark-field TEM image; (D) STEM image and EDS profile.

tion−dehydrogenation experiment (in hydrogenated state), respectively. It shows that the grain size of the mixture was almost unchanged and TiH_2 was still distributed uniformly among the MgH_2 particles. This result is similar to a previous

report by Friedrichs et al.[55] which showed that the addition of Nb_2O_5 hinders the MgH_2 from grain growth during the heating process.

5. Conclusions

It is concluded based on the results of this study that a nanostructured uniform mixture of $MgH_2-0.1TiH_2$ powder prepared by ultrahigh-energy−high-pressure reactive milling is a reversible hydrogen storage material with a cyclic hydrogen storage capacity of 6 wt %. The hydrogenation and dehydrogenation kinetics are rapid at 290 °C. The material demonstrated a high cycle stability with no loss of capacity over 80 cycles. Further, HRTEM and STEM analysis showed that the grain size of the milled $MgH_2-0.1TiH_2$ powder is approximately 5−10 nm with TiH_2 distributed uniformly among the MgH_2 particles. The results demonstrate that both the nanosize and the addition of TiH_2 contribute to the improvement of the kinetics of dehydrogenation and hydrogenation of MgH_2. The results also show that the ΔH value of the dehydrogenation of $MgH_2-0.1TiH_2$ is lower than that of MgH_2. The ΔS value is, however, also lower than that of commercial pure MgH_2.

Acknowledgment. This research was supported by the U.S. Department of Energy (DOE) under contract number DE-FC36-05GO15069. The authors thank Mr. Vineet Kumar for his assistance with the TEM analysis.

JA906340U

(55) Friedrichs, O.; Aguey-Zinsou, F.; Ares Fernandesz, J. R.; Sanchez-Lopez, J. C.; Justo, A.; Klassen, T. *Acta Mater.* **2006**, *54*, 105.